Simulation of Past Changes in the Austrian Snow Cover 1948–2009

THOMAS MARKE

University of Innsbruck, Innsbruck, Austria

FLORIAN HANZER

University of Innsbruck, Innsbruck, and Wegener Center for Climate and Global Change, Graz, Austria

MARC OLEFS

Zentralanstalt für Meteorologie und Geodynamik, Vienna, Austria

ULRICH STRASSER

University of Innsbruck, Innsbruck, Austria

(Manuscript received 21 December 2017, in final form 7 August 2018)

ABSTRACT

A distributed snow model is applied to simulate the spatiotemporal evolution of the Austrian snow cover at 1 km × 1 km spatial and daily temporal resolution for the period 1948–2009. After a comprehensive model validation, changes in snow cover conditions are analyzed for all of Austria as well as for different Austrian subregions and elevation belts focusing on the change in snow cover days (SCDs). The comparison of SCDs for the period 1950–79 to those achieved for 1980–2009 for all of Austria shows a decrease in SCDs with a maximum of >35 SCDs near Villach (Carinthia). The analysis of SCD changes in different subregions of Austria reveals mean changes between −11 and −15 days with highest absolute change in SCDs for southern Austria. Two decrease maxima could be identified in elevations of 500–2000 m MSL (between −13 and −18 SCDs depending on the subregion considered) and above 2500 m MSL (over −20 SCDs in the case of central Austria). The temporal distribution of SCD change in the Austrian subregions is characterized by a reduction of SCDs in midwinter and at the end of winter rather than by fewer SCDs in early winter. With respect to the temporal distribution of SCD change in different elevation belts, changes in elevations below 1000 m MSL are characterized by a distinct reduction of SCDs in January. With increasing elevation the maximum change in SCDs shifts toward the summer season, reaching a maximum decrease in the months of June–August above 2500 m MSL.

1. Introduction

Snow depth and snow cover duration in the Alps are characterized by a high interannual to decadal variability indicating a high sensitivity to climatic conditions and climatic change. Changes in the spatial and temporal evolution of the Alpine snow cover are of high relevance as the temporal storage of water in the snowpack and the delayed water release in spring strongly affect hydrological conditions in Alpine watersheds, for example, through a modification of soil moisture conditions, evapotranspiration, and runoff generation, as well as its timing and magnitude (Kane et al. 1991; Hinzman et al. 1996; Marsh 1999; Luce et al. 1998). Beside its importance for water availability in downstream regions, where meltwater is required for domestic, industrial, or agricultural applications (see Barnett et al. 2005), snow availability and reliability further represent preconditions for snow-related sport activities and hence are key factors for Alpine winter tourism (EEA 2012). But snow is not only a key factor for water availability and economy, but also plays an important role for the natural environment of the Alps, as the presence or absence of a snow cover dominates the vegetation cycle. In consequence, changes in the snow cover can result in shifts in the species distribution of plants (Keller et al. 2005). Finally, the presence or absence of a snow cover also affects weather and climate as the special

Corresponding author: Thomas Marke, thomas.marke@uibk.ac.at

DOI: 10.1175/JHM-D-17-0245.1

characteristics of a snow surface (e.g., its albedo or temperature) regulate the shortwave and longwave radiation balance with the respective effects on near-surface air temperatures (Jin and Miller 2007).

Although the multifaceted importance of the Alpine snow cover for nature and economy is well known, studies on climate change impacts on the spatiotemporal snow cover evolution in Austria are sparse. Hantel et al. (2000) analyzed observed days with snow cover and air temperature for 84 stations in Austria in 1961–90 to investigate the sensitivity of snow cover days on European air temperature. Their study indicates that middle-elevation sites are most sensitive to temperature change, with a suggested decrease in the length of the snow cover period of approximately 4 weeks in winter and 6 weeks in spring as a result of a temperature increase of 1 K. Schöner et al. (2009) carried out an analysis of snow depth observations at Sonnblick Observatory (Austria) dating back to 1928 in order to investigate the temporal snow variability at an high-Alpine site, but with naturally limited spatial transferability of the achieved results. Besides the cited studies based on snow station records, there are further studies investigating the spatiotemporal evolution of the Austrian snow cover using remote sensing data. Satellite products like the Moderate Resolution Imaging Spectroradiometer (MODIS) snow cover product provide valuable snow cover information that supplements snow depth recordings, particularly in regions with sparse observations (Parajka and Blöschl 2008b). While the accuracy of the MODIS snow cover product is generally very high (Parajka and Blöschl 2006, 2008a; Hall and Riggs 2007) and satisfies the requirements of most snow cover studies, the fact that clouds often obscure the snow-covered surfaces somehow limits its potential (Parajka and Blöschl 2006). Hüsler et al. (2014) have derived a 1-km satellite-based snow cover dataset for the Alpine region from Advanced Very High Resolution Radiometer (AVHRR) data. This dataset was used to examine the spatiotemporal distribution of snow cover in the European Alps for the years 1985–2011. Their study reports a significant decrease in the snow cover duration at lower elevations in the southeastern and southwestern regions of the Alps with no significant trend in the monthly mean snow covered area during the time period considered. As an important issue of future work, these authors formulate a clear need for studies analyzing seasonal changes in the snow cover evolution.

While most existing historical analyses of snow cover variability and trends make use of local station recordings of meteorological/snow variables or remotely sensed snow information, there are only a few studies applying spatially distributed models. The latter can provide spatially and temporally highly resolved information on patterns of snow cover dynamics, if desired, even for potential future climate conditions, by coupling the snow model to climate change scenarios. A numerical simulation of natural and artificial snow conditions for past and potential future climate conditions has been carried out by Marke et al. (2015) for IPCC A1B scenario conditions in a representative skiing destination in Styria (Austria). This study again only considers an area of very limited extent and lacks spatial transferability. Moreover, the achieved results are based on coupled GCM–RCM simulations and hence include all uncertainties incorporated in assumptions underlying the climate scenarios, the choice of the climate scenarios/realizations and uncertainties inherent in the climate simulations themselves. None of the studies cited provide a complete picture of climate change impacts on Austrian snow conditions as already experienced in the past. In contrast to Austria, where an extensive study on spatiotemporal changes of snow cover is still missing, several studies on past snow cover variability and changes exist for Switzerland (e.g., Beniston 1997; Beniston et al. 2003a,b; Beniston 2012; Laternser and Schneebeli 2003; Scherrer et al. 2004; Marty 2008; Serquet et al. 2011; Klein et al. 2016; Marty et al. 2017). Most of these studies report a decrease of the snow depth since the mid-1980s for stations in lower elevations. Analyzing the number of snow cover days at 34 stations in Switzerland for the years 1948–2007, Marty (2008) found a stepwise decrease at the end of the 1980s followed by an unprecedented series of low-snow winters in the last 20 years of the considered period. Similar results were achieved by Klein et al. (2016), who investigated changes in snow cover duration at 11 meteorological stations in different elevations in Switzerland for the period 1970–2015. Besides snow depth, changes are also reflected in an observed decrease of snow mass: Marty et al. (2017) recently found a region-independent reduction of snow water equivalent in the Swiss Alps driven by increasing temperatures and a coincident weak reduction of precipitation.

To provide a sophisticated analysis of spatiotemporal changes in past snow cover conditions in Austria, we apply a numerical snow model for simulating snow conditions at a spatial resolution of 1 km × 1 km and a temporal resolution of one day over the period 1948–2009. Compared to most of the studies already cited, this approach comes along with various advantages. First, studies carried out with point-scale snow cover observations often suffer from inhomogeneities in the underlying time series that result from gaps in the snow records or from the dislocation of the point of observation over time. These shortcomings can be avoided using a spatially distributed snow model, as such a model provides temporally continuous simulations of snow conditions for every grid cell in the model domain.

Second, spatially consistent simulation of snow conditions supplements snow cover observations available for single sites in Austria and compensates for the unrepresentativeness of snow data for all areas but the sites of measurement themselves. Third, spatially distributed snow simulations cover the whole range of elevation levels in Austria and complement the estimated snow conditions particularly in higher elevations, where snow observations are sparse.

The target variable of our study is the snow cover day (SCD), which represents an adequate indicator for snow conditions in a given winter. It is directly derived from snow cover simulations by counting the days with a simulated snow depth greater 1 cm. Changes in SCDs are separately discussed for all of Austria and four Austrian subregions. Within the subregions, changes in snow conditions are separately investigated for different elevation belts. With our modeling results we present for the first time a continuous snow climatology for the period 1948–2009 and all of Austria. We provide a spatially and temporally consistent picture of past changes in the Austrian snow cover evolution on the example of simulated SCDs. The main research questions to be addressed in this study are:

- How did the natural snow cover in Austria respond to climatic changes in the past?
- How does this response vary spatially, for example, for different regions and elevation levels in Austria?

2. Materials and methods

a. Study area

In the present study, we investigate spatiotemporal changes in the snow cover evolution for all of Austria and for four different subregions separately. Austria is located in central Europe with a total area of 83 810 km^2 [derived from the 1 km × 1 km digital elevation model (DEM) used in this study]. The four subregions considered each share a common variance in the time-dependent evolution of snow time series and have been defined using empirical orthogonal functions (EOFs; see Fig. 1) [for additional details on the subregion delineation, see Schöner et al. (2017, manuscript submitted to *Int. J. Climatol.*)]. Climatically, the study area is characterized by a mean annual temperature of 6.5°C, with the subregions characterized by mean temperatures of 3.6°C (western Austria), 4.8°C (southern Austria), 5.1°C (central Austria), and 8.7°C (northeastern Austria). Mean annual precipitation in Austria amounts to 1159 mm, with the subregions receiving 1482 (western Austria), 1276 (southern Austria), 1387 (central Austria), and 907 mm (northeastern Austria) in a multiyear average. The values presented here have been derived from the spatially refined station recordings in Austria for the period 1950–2009 as used in this study as input for the snow model. Following the updated Köppen–Geiger climate classification published by Kottek et al. (2006), the northeastern part of Austria is mainly represented by a Cfb type, defined as a warm temperate, fully humid climate with warm summers. The central and southern Austrian subregion are both characterized by Dfb climate in the eastern part and a Dfc climate in the western part of the respective subregion, with both types representing a fully humid snow climate, with a warm (mean temperature in the warmest month < 22°C and at least 4 months with mean temperatures > 10°C) and cool (less than 4 months with mean temperatures > 10°C and coldest month with average temperatures > -38°C) summer, respectively. In western Austria different climates from Cfb over Dfc to Dfb types can be found. Because of their warmest months with mean temperatures between 0° and 10°C, the higher elevated regions of western and central Austria fall into the ET category, representing a polar tundra climate.

With respect to climate change, the temperature increase in Austria with 2 K since 1880 is far above the global average (0.85 K; APCC 2014). Thereby, the most distinct increase is observed in the period after 1980, in which temperatures increased by approximately 1 K (APCC 2014). The change in precipitation over the last 150 years is characterized by significant regional differences. While in western Austria an increase in annual precipitation of approximately 10%–15% is observed, precipitation in the southeast decreased in a similar order of magnitude (APCC 2014).

b. Model description

The spatially distributed snow model Alpine Multiscale Numerical Distributed Simulation Engine (AMUNDSEN; Strasser 2008) is applied in the present study for simulating the Austrian snow cover. The model has been designed to specifically address the requirements of snow modeling in mountain regions under climate change conditions (Strasser et al. 2004, 2008; Strasser 2008; Marke et al. 2015). For the present study, it has been adapted to operate at daily time steps using temperature and precipitation as meteorological input data only. For the consideration of topographic effects (e.g., orographic shadowing) the model requires a DEM, with a resolution of 1 km × 1 km chosen for the simulations in this study. In each model time step, a meteorological preprocessor in AMUNDSEN is used to regionalize the meteorological point information from the station locations to the model domain.

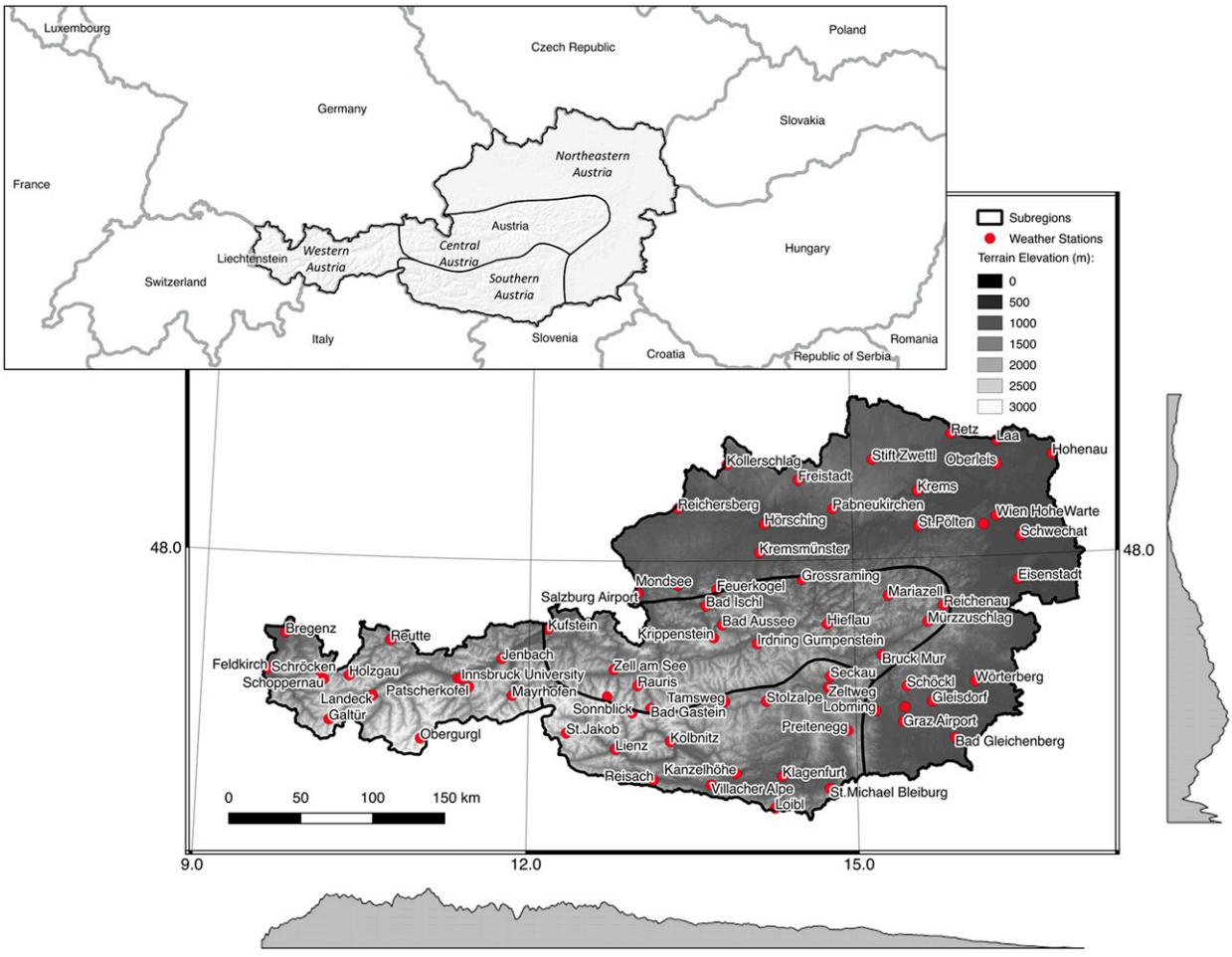

FIG. 1. Overview of the study area showing the spatial distribution of terrain elevation for Austria (1 km × 1 km resolution), the location of the weather stations providing input for the snow simulations (red dots, status 2009), and the different subregions separately discussed in this study (black lines). The gray areas on the bottom and the right show the relative distribution of elevation derived from the mean elevation in the *x* and *y* directions.

Topographic corrections for precipitation and temperature are carried out by applying prescribed monthly altitudinal corrections as described by Liston and Elder (2006) and Marke (2008). Thereby, the recorded temperature values are first transformed to a common reference level (defined as sea level) using the station elevation and predefined monthly temperature lapse rates. The latter have been derived from 221 weather stations in Austria and Germany by Marke (2008). These temperatures at reference level are spatially interpolated and then corrected for the actual terrain elevation using a DEM in 1 km × 1 km resolution in combination with the monthly lapse rates. The topographic correction of precipitation as first proposed by Thornton et al. (1997) follows a similar approach, with the exception that a nonlinear correction function is applied and that the reference level here is the interpolated elevation of the weather stations to account for the nonlinear character of the applied elevation adjustment function (Liston and Elder 2006). The precipitation adjustment factors applied in the nonlinear altitudinal correction have again been taken from Marke (2008).

After interpolation, precipitation phase is determined. To account for the fact that humidity data were not available far back in the past (as would be required for phase detection based on a wet-bulb temperature threshold), the classical method of determining precipitation phase from air temperature alone was implemented in AMUNDSEN for this study. As also described by other authors (e.g., Harpold et al. 2017), two temperature thresholds define the temperature range in which mixed precipitation occurs (with linear interpolation of the rain/snow fraction in between), while below and above these thresholds precipitation is assumed to be only snow and

TABLE 1. Calibrated parameter values used in the model simulations.

Parameter	Value	Description
T_{snow}	0°C	Lower limit for snow–rain partitioning
T_{rain}	2°C	Upper limit for snow–rain partitioning
SCF	1.2	Snow correction factor
TF	3 mm day^{-1} °C^{-1}	Temperature factor for snowmelt calculation
SRF	0.02 m^2 mm day^{-1} W^{-1}	Radiation factor for snowmelt calculation
T_T	1°C	Threshold temperature for snowmelt calculation

rain, respectively. To account for the undercatch of solid precipitation recorded at precipitation gauges, a prescribed snow correction factor was applied on the station time series prior to interpolation. This factor was determined by calibration based on the simulated snow cover evolution as well as glacier mass balance at different Austrian sites (see Table 1 for calibrated parameter values).

The conversion of simulated snow water equivalent (SWE) to snow depth distinguishes between two types of snow layers, called ''new snow'' and ''old snow'' (see Marke et al. 2015; Hanzer et al. 2016). The density of freshly fallen snow is calculated as a function of air temperature while snow compaction is calculated separately for each layer [Eqs. (1)–(3)]. A phase of rapid compaction for newer snow (to simulate destructive metamorphism) is thereby followed by a phase of slower densification mainly influenced by the snow load:

$$\frac{d\rho_s}{dt} = \rho_s(c_1 W^* e^{-c_2(T^*-T_s)} e^{-c_3\rho_s}), \tag{1}$$

$$\frac{d\rho_s}{dt} = \rho_s(c_4 e^{-c_5(T^*-T_s)} c_6), \tag{2}$$

$$c_6 = \begin{cases} e^{-c_7(\rho_s-\rho_d)}, & \rho_s > \rho_d \\ 1, & \rho_s \le \rho_d, \end{cases} \tag{3}$$

with ρ_s (kg m^{-3}) being the layer (new snow or old snow) density, W^* (kg m^{-2}) the load of snow water equivalent (snow in the layer above and 50% of the snow in the current layer), $c_1 = 0.01$ m^{-1} h (new snow), $c_1 = 0.001$ m^{-1} h (old snow), $c_2 = 0.08$°C^{-1}, $c_3 = 0.021$ m^3 kg^{-1}, $c_4 = 0.01$ m^{-1} h, $c_5 = 0.04$°C^{-1}, $c_7 = 0.046$ m^3 kg^{-1} $\rho_d = 150$ kg m^{-3} and $T^* = 0$°C.

New snow is converted to old snow when reaching a threshold density of 200 kg m^{-3}. Snow albedo is parameterized using an aging curve approach taking snow age and air temperature into account (Rohrer 1992).

Since the meteorological input data in terms of variables and resolution do not allow a fully physically based simulation of the snow surface energy balance, an enhanced temperature index approach considering potential shortwave radiation is applied. The applied approach is similar to the one developed by Pellicciotti et al. (2005), but operates at daily instead of hourly time steps and utilizes potential instead of actual solar radiation [see Eq. (4)]. The latter modification was necessary as recordings of solar radiation in Austria do not reach back far in the past. Snowmelt M (mm day^{-1}) is calculated as a function of mean daily air temperature T (°C) as well as snow albedo α and daily sums of potential clear-sky incoming broadband solar radiation I (W m^{-2}):

$$M = \begin{cases} \mathrm{TF}(T - T_T) + \mathrm{SRF}(1-\alpha)I, & T > T_T \\ 0, & T \le T_T. \end{cases} \tag{4}$$

The threshold temperature for snowmelt T_T (°C) as well as the temperature factor TF (mm day^{-1} °C^{-1}) and solar radiation factor SRF (m^2 mm day^{-1} W^{-1}) are calibration parameters. For calibration, the model was run using 10 000 random parameter sets generated assuming uniform distribution within the prescribed parameter ranges. The parameter set used for the results presented in this study (see Table 1) was then selected based on the objective function to maximize the Nash–Sutcliffe efficiency of observed versus simulated snow depth at 24 stations with available long-term snow measurements.

To avoid inhomogeneities in the model results arising from a strongly varying number of meteorological stations due to 1) gaps in the recorded temperature and/or precipitation time series as well as 2) dislocation of weather stations in the observation period, we only applied homogenized measurements (Auer et al. 2010; Nemec et al. 2013) available for a minimum of 45 years for the meteorological model input in this study. As a sufficiently large number of meteorological stations with homogenized measurements of temperature and precipitation was only available starting from 1948: model runs were performed for the period 1948–2009. The number of available homogenized temperature (precipitation) time series increased from 46 (35) in 1948 to 70 (59) from 1961 to 1999, slightly declining to 60 (50) in 2009 (Fig. 1). Reducing the number of meteorological stations to only those constantly available over the whole time period considered would have reduced the uncertainty from a varying station number. However,

the low number of constantly available stations would have negatively affected model performance and, as a result, the robustness of the findings related to snow cover change.

The SCDs for a given winter season and location are calculated as described by Eq. (5) as the number of days with a snow depth (HS) exceeding 1 cm and are derived as

$$\mathrm{SCD} = \sum_{i=1}^{N} S_i, \tag{5}$$

where N is the number of days in the season and

$$S_i = \begin{cases} 1, & \mathrm{HS}(i) > 1\,\mathrm{cm} \\ 0, & \mathrm{HS}(i) \le 1\,\mathrm{cm}. \end{cases} \tag{6}$$

c. Validation approach

Validation of the model results is performed both by comparing time series of daily snow depth and annual SCDs against the respective observations at the locations of the meteorological stations and by comparing the respective model results to satellite-derived binary snow extent maps. Thereby, different efficiency criteria are considered to evaluate model performance [see Eqs. (7)–(11)]. The Nash–Sutcliffe model efficiency (NSME), which is among the criteria often recommended for validation in environmental modeling studies (Richter et al. 2012; Krause et al. 2005), ranges between $-\infty$ and 1, with a perfect fit having a value of 1. It is calculated as

$$\mathrm{NSME} = 1 - \frac{\sum_{i=1}^{n} (O_i - S_i)^2}{\sum_{i=1}^{n} (O_i - \overline{O})^2}, \tag{7}$$

where O_i and S_i denote the observations and simulations at time step i, respectively.

The percent bias (PBIAS) indicates the general model tendency toward over- or underestimating the observed values (a perfect fit having a value of 0). It is calculated in form of

$$\mathrm{PBIAS} = 100 \frac{\sum_{i=1}^{n} (S_i - O_i)}{\sum_{i=1}^{n} O_i}. \tag{8}$$

The mean error (ME), mean absolute error (MAE), and mean absolute percentage error (MAPE), all having an ideal value of 0, are calculated as

TABLE 2. A 2 × 2 contingency table for the comparison of binary snow cover observations and simulations (after Zappa 2008). Variables O and S denote observations and simulations, while the subscripts 0 and 1 correspond to snow-free and snow-covered situations, respectively.

	S_1	S_0	Σ
O_1	n_{11}	n_{01}	n_{x1}
O_0	n_{10}	n_{00}	n_{x0}
Σ	n_{1x}	n_{0x}	n_{xx}

$$\mathrm{ME} = \frac{1}{n} \sum_{i=1}^{n} S_i - O_i, \tag{9}$$

$$\mathrm{MAE} = \frac{1}{n} \sum_{i=1}^{n} |S_i - O_i|, \quad \text{and} \tag{10}$$

$$\mathrm{MAPE} = \frac{100}{n} \sum_{i=1}^{n} \left| \frac{S_i - O_i}{O_i} \right|. \tag{11}$$

For the comparison of the model results to satellite-derived snow cover maps, the contingency-table-based criteria accuracy (ACC) and bias (BIAS) are used (Table 2). The accuracy ACC is the number of correctly simulated grid cells divided by the total number of cells with values between 0 and 1, with 1 representing a perfect match between the two datasets [see Eq. (12)]. BIAS represents the frequency of correct snow predictions ranging between 0 and ∞; again, a value of 1 is a perfect match [see Eq. (13)]. The criteria are calculated as

$$\mathrm{ACC} = \frac{n_{11} + n_{00}}{n_{xx}}, \tag{12}$$

$$\mathrm{BIAS} = \frac{n_{1x}}{n_{x1}}. \tag{13}$$

Values less than 1 of BIAS indicate underestimations of the simulated snow cover extent, whereas values greater than 1 indicate overestimations. For the definitions of n_{00} to n_{xx} see Table 2.

d. Remote sensing data

Satellite-based snow cover products like those of MODIS mounted on the *Aqua* and *Terra* satellites represent a valuable source of information to be applied for the spatiotemporal analysis of snow cover evolution (Hüsler et al. 2014) or for validation of snow models (Hanzer et al. 2016). Parajka and Blöschl (2006) have evaluated the MODIS snow cover product for the territory of Austria. They report that the classification accuracy is very good for cloud-free days (95%). However, for the analysis of the spatiotemporal variability of the

MODIS snow cover, the fact that clouds on average obscure the Austrian territory by 63% is argued to clearly limit the potential of snow products derived from optical sensors (Parajka and Blöschl 2006). While Parajka and Blöschl (2008a) have shown that filtering techniques can contribute to cloud reduction, their study has also identified a clear trade-off between cloud coverage and mapping accuracy. As described by Hall and Riggs (2007), the accuracy of the MODIS snow cover product varies for different land cover types, topographic conditions, and the time of acquisition (time of the day and season). For forested areas and complex terrain as well as for thin snow (<1 cm) and ephemeral snow conditions, a lower accuracy is suggested. Here, we use the threshold of HS > 1 cm for the definition of a simulated SCD [see Eq. (5)] to minimize deviations between the MODIS data and model results that arise from snow classification errors or differing definitions for the presence of a snow cover. Parajka and Blöschl (2008a) show that the overestimation error in snow cover detected by MODIS increases with elevation reaching up to 15% in elevations above 1500 m MSL in the winter months, whereas no correlation between elevation and underestimation errors could be identified. Compared to the *Terra* snow maps, the corresponding *Aqua* products have been less intensively validated in the past; however, available studies indicate that the accuracy of the *Aqua* snow products appears to be lower, at least in forested areas (Hall and Riggs 2007). As discussed by Hall and Riggs (2007), the confusion of clouds and snow introduces the largest uncertainty in the MODIS snow products. In particular, the concurrent presence of snow and rock/soil in a single MODIS raster cell results in a spectral signature in the shortwave infrared range that can be similar to that of clouds (Rittger et al. 2013). Another factor that introduces uncertainty in MODIS snow cover products is dirt or soot on the snow cover. These deposits lower the normalized difference snow index (NDSI) due to their effect on the visible portions of the reflectance spectrum. In consequence, this leads to an underestimation of snow in the remotely sensed data (Rittger et al. 2013).

For the spatial validation of simulated SCDs in this study, the daily 500-m-resolution NASA MODIS snow cover products MOD10A1 (*Terra*) and MYD10A1 (*Aqua*) in version 5 (Hall et al. 2002) have been considered. The *Terra* and *Aqua* scenes for each day were merged into composite images using the approach described in Hanzer et al. (2016) and resampled to the 1-km resolution of the snow model using mode resampling (i.e., choosing the most common value within the respective 2 × 2 windows). Validation of observed and simulated snow cover is performed both space integrated (i.e., averaging over all pixels for a given date) and time integrated (i.e., averaging over all available dates for each pixel). For the former, a maximum cloud coverage criterion of 25% over the entire region was taken into account, resulting in a total of 277 satellite scenes for the period 2000–09 (November–April), while for the latter for each pixel between 501 and 837 scenes (where the respective pixel is cloud-free) were available.

3. Results

a. Validation results

Prior to the analysis of simulated SCDs, the applied model setup has been validated thoroughly. Figure 2 shows the snow cover simulations in comparison to observations at several sites chosen to represent different elevation levels in Austria for the period 1990–2000. While for some stations and/or years larger deviations between observed and simulated snow depths occur (particularly at higher elevated sites like station Villacher Alpe), the general course of snow accumulation and ablation seems well reproduced by the model. As in higher elevations the SCDs derived from simulated snow depth are less sensitive to a correct representation of snow depths throughout the winter season than to an accurate simulation of the beginning and the end of the snow cover period, the accuracy of simulated SCDs can be high there even in years where the simulated snow depth differs significantly from the observations. At lower elevations where the snow cover is less continuous, the accuracy of simulated SCDs strongly depends on an accurate reproduction of (often little) snow depths, resulting in relatively large differences between simulated and observed SCDs. Snow depth generally seems well reproduced.

A more detailed picture of model performance at an extended set of sites in Austria is given in Table 3. While the MAE in simulated snow depth increases with station elevation due to higher snow amounts and lateral wind-induced snow redistribution, the resulting values of the NSME between 0.33 and 0.81 suggest satisfactory model performance for the full range of elevations. SCDs are less sensitive to biases in higher snow depth ranges, due to their nature as a threshold-based criterion [number of days with snow depth greater 1 cm; see Eq. (5)]. The small average ME and MAE in simulated SDCs of −4.8 and 14 days, respectively, confirm the satisfactory performance with respect to the simulation of SCD as snow indicator. Highest deviations between simulated and observed SCDs can be observed for midelevations where the land surface is less continuously snow-covered or snow-free compared to elevations above and below.

To evaluate the model performance with respect to the reproduction of spatial snow cover evolution, a comparison between simulated and observed (i.e., remotely

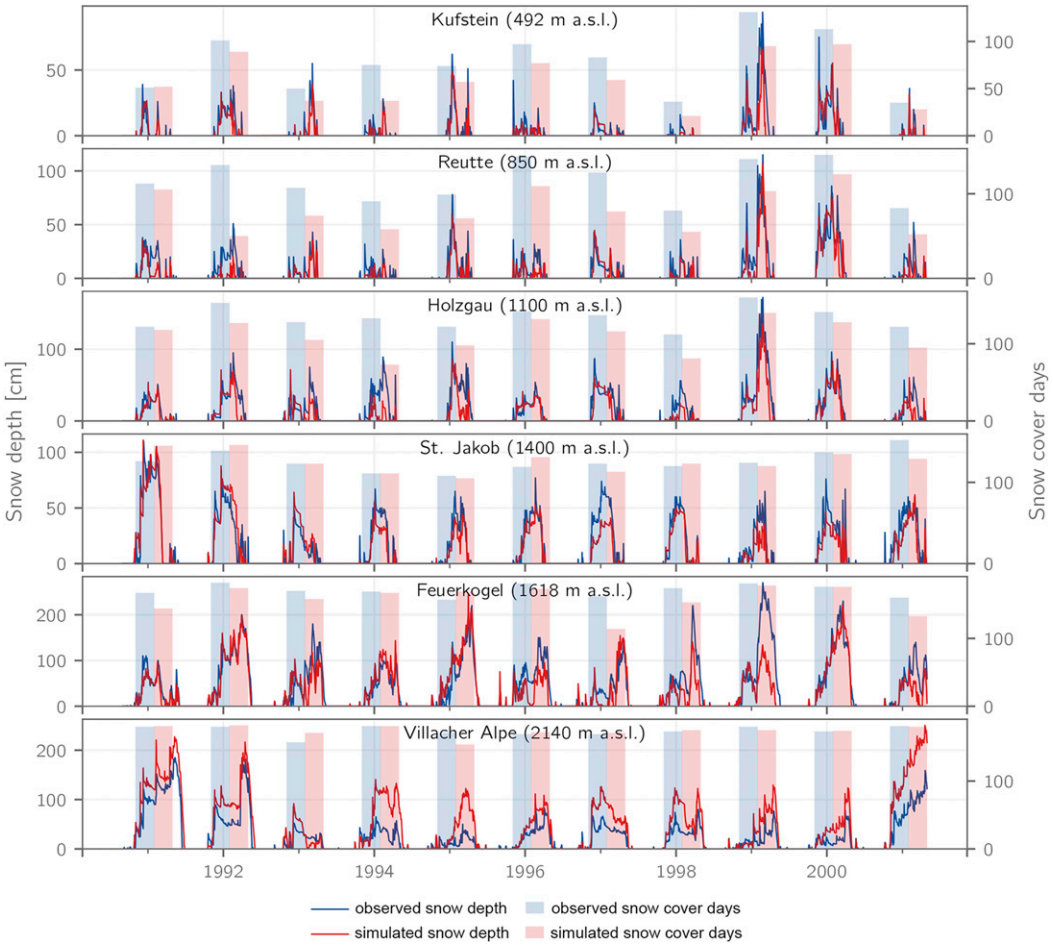

FIG. 2. Comparison of observed and simulated daily snow depth (lines) and seasonal (November–April) snow cover days (bars) at different sites in Austria for the period 1990–2001.

sensed) snow-covered area has been carried out for a series of dates with available snow distribution from the NASA MODIS snow cover product (see section 2; Hall et al. 2002). Figure 3 shows the results of this comparison for the two statistical criteria: accuracy and bias. The temporal evolution of these two criteria as shown in Fig. 3 reveals that ACC with values from 0.7 to 1.0 is high throughout the winter while BIAS values of below 0.5 at the beginning of the winter season indicate a certain underestimation of snow cover conditions in early winter. Figure 4 shows the same efficiency criteria calculated in a time-integrated rather than space-integrated manner for the territory of Austria. With a mean ACC of 0.83 and a mean BIAS of 0.84, these results again confirm that the model performs well in the simulation of snow cover distribution for Austria, with a tendency to underestimate SCDs by 16%. Considering ACC values for different elevation belts (see line plot in the upper left of the ACC plot illustrated in Fig. 4), lowest values again are derived for midelevations (1000–1500 m MSL). The corresponding BIAS values show an underestimation of SCDs below these midelevated regions, and an overestimation above. An explanation for lower elevations showing relatively high ACC values but relatively low BIAS values is given by the fact that BIAS only considers the raster cell values correctly classified as snow, while ACC considers all correctly classified raster cell values, including snow-free conditions [see Eqs. (12) and (13)]. As lower elevations are often snow-free and the model seems to reproduce these conditions with good accuracy, this consideration of snow-free conditions positively affects the values of ACC in these elevations.

b. *Change in snow cover days*

Using the previously described model setup, AMUNDSEN was applied to produce daily maps of SWE, snow depth, and snowmelt for the period 1948–2009. Figure 5 shows the average number of SCDs calculated

TABLE 3. Skill scores for the comparison of observed and simulated snow depth for selected stations in Austria and the period 1970–2009 [winter half year (November–April) only], as well as mean annual observed and simulated SCDs. The skill scores shown are the ME, MAE, NSME, PBIAS, and MAPE.

Station	m MSL	MAE (cm)	NSME	PBIAS (%)	$SCDs_{obs}$	$SCDs_{sim}$	ME_{SCD} (days)	MAE_{SCD} (days)	$MAPE_{SCD}$ (%)
Wien Hohe Warte	203	0.59	0.67	−27.5	37	43	6.3	8.7	38.1
Graz University	366	0.56	0.75	−18.9	39	45	6.6	9.0	38.7
Kremsmuenster	383	1.03	0.48	18.9	52	64	11.4	11.9	31.1
Bregenz	424	0.72	0.59	−37.6	44	38	−5.9	10.4	73.0
Salzburg Airport	430	0.75	0.60	−25.0	53	54	0.8	7.4	19.2
Feldkirch	440	0.76	0.45	−27.6	47	41	−5.5	8.5	40.5
Klagenfurt	450	1.44	0.70	−1.9	65	72	7.4	12.8	66.9
Mondsee	491	1.70	0.42	18.4	58	61	3.0	9.4	20.0
Kufstein	492	1.91	0.80	−13.0	82	76	−5.9	11.6	18.6
Jenbach	530	1.38	0.78	−29.9	65	60	−5.6	9.1	17.9
Mayrhofen	643	2.46	0.62	12.2	98	91	−7.3	11.2	12.2
Lienz	659	2.46	0.81	−12.0	83	84	0.8	9.8	16.1
Landeck	798	1.25	0.60	−6.9	61	63	2.4	10.4	32.6
Reutte	850	4.04	0.67	−41.9	121	90	−30.9	30.9	26.1
Loibl	1098	7.34	0.71	−22.8	136	112	−24.0	24.0	18.9
Holzgau	1100	6.86	0.72	−23.6	139	129	−9.4	31.5	22.7
St. Jakob	1400	4.90	0.81	−22.9	136	135	−0.2	10.2	8.1
Kanzelhoehe	1526	6.62	0.72	−35.3	143	131	−12.2	15.1	10.6
Feuerkogel	1618	16.43	0.78	−23.0	194	178	−15.6	16.9	8.9
Obergurgl	1938	14.63	0.52	−45.0	187	163	−24.4	24.8	13.3
Villacher Alpe	2140	20.09	0.33	60.9	206	217	11.2	13.7	7.0
Patscherkofel	2247	15.52	0.66	−29.8	216	209	−7.5	11.0	5.1
Mean	919	5.16	0.65	−15.2	103	98	−4.8	14.0	24.8

for all of Austria and the period 1950–2009. Because of the vertical temperature gradient, the spatial representation of SCD reveals a strong correlation with altitude resulting in highest SCD values on the order of 365 days in highest elevations. The average number of SCDs gradually decreases, with altitude reaching a minimum of approximately 25 days in the lower elevations of the valley floors and the northeastern and southern part of Austria.

Figure 6 shows the difference in the mean simulated number of annual SCDs between the period 1950–79 and 1980–2009. As can be seen for most parts of Austria, SCDs strongly decrease, with a maximum decrease of >35 days near Villach (Carinthia). The comparison of the mean annual SCDs simulated for the four Austrian subregions considered for the period 1950–79 to the conditions simulated for the period 1980–2009

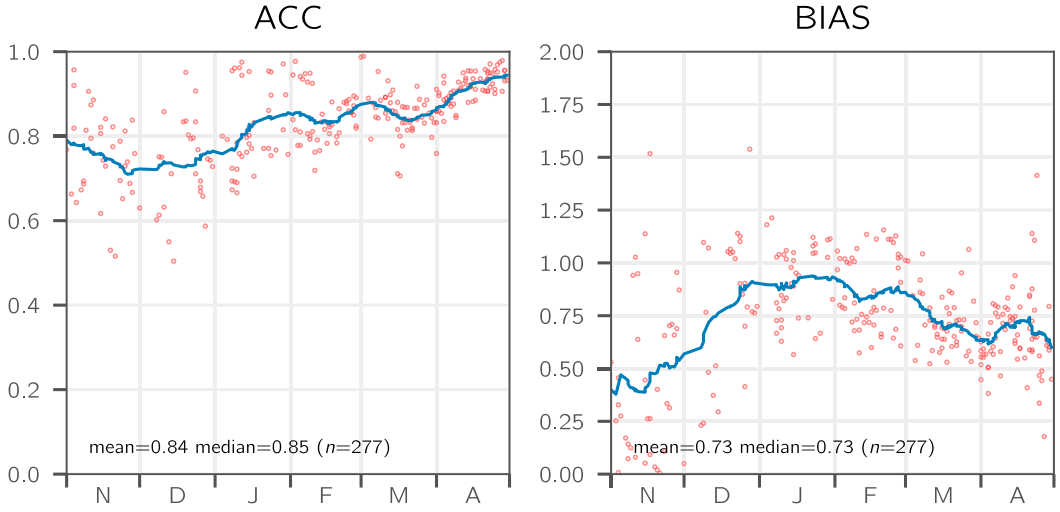

FIG. 3. Temporal evolution of the (left) ACC and (right) BIAS derived by comparison of simulated snow cover to a total number of 277 satellite scenes. The blue lines indicate the 30-day running mean.

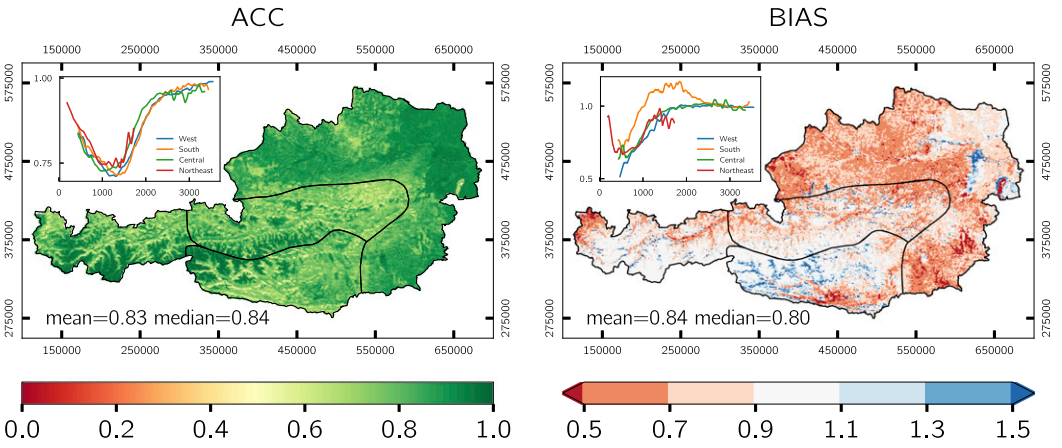

FIG. 4. Spatially distributed (left) ACC and (right) BIAS yielded by comparison of simulated snow cover to all available cloud-free MODIS scenes on a pixel basis for the winter half year (November–April). The line plots in the upper-left corners show the average ACC and BIAS values as a function of elevation for the four subregions.

(see Table 4) reveals changes ranging from −11 to −15 days. The provided values here represent the mean values of all model grid cells in the respective region. While the lowest absolute decrease with 11 days is calculated for northeastern Austria, this region is subject to the highest percent decrease (−17%) due to the low number of snow cover days in the reference period 1950–79.

To analyze changes in SCDs separately for different elevation levels, the DEM used for the snow simulations was divided into elevation belts of 100-m width. As Fig. 7 reveals, the decrease in SCDs intensifies from very low elevations (<500 m MSL) toward midelevations (500–2000 m MSL), followed by a certain tendency to lower reduction in SCDs in elevations of approximately 2500 m MSL. In elevations between 500 and 2000 m MSL, the maximum decrease in SCDs ranges from −13 (central Austria) to −18 SCDs (southern Austria). For elevations above 2500 m MSL, a second decrease maximum can be observed, with values exceeding −20 SCDs in the case of central Austria. The fact that the decrease in SCDs in lowest elevations is below that in higher elevations can be explained by the low number of SCDs and the consequently low potential for decrease in low elevations.

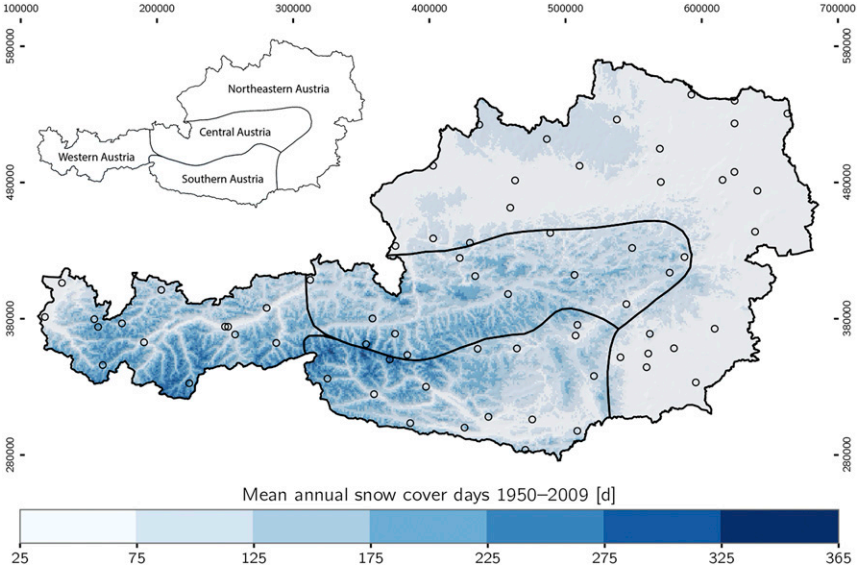

FIG. 5. Simulated snow cover days for the period 1950–2009. The black contours delineate the four Austrian subregions. Dots mark the station network supplying the meteorological input for the simulations (status 2009).

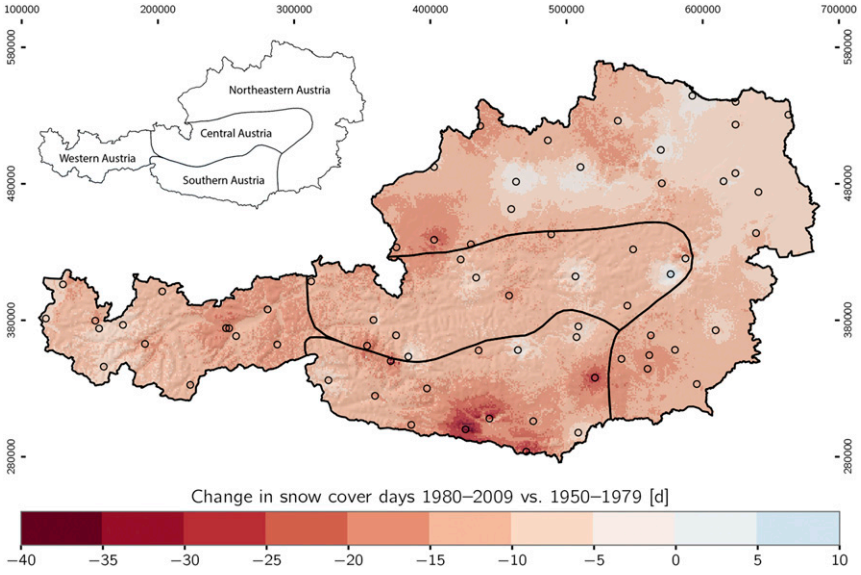

FIG. 6. Change in snow cover days 1950–79 vs 1980–2009. The black contours delineate the four Austrian subregions. Dots mark the station network supplying the meteorological input for the simulations (status 2009).

Figure 8 shows the mean monthly SCDs for the two periods and all subregions considered. The decrease in SCDs for all subregions is rather due to a severe reduction in SCDs in midwinter and at the end of winter, than to reduced SCDs in early winter.

Analyzing the seasonal changes in SCDs in different elevation levels (see Fig. 9) reveals that in elevations below 1000 m MSL, the most distinct change in SCDs is due to a reduction of SCDs in January. This is found for all four Austrian subregions considered, with only the values in December falling below the January values in western Austria. Above 1000 m MSL, the largest change in SCDs is shifting toward the end of the winter season (or even summer) with increasing elevation, with a maximum decrease in the months of June to August in elevations above 2500 m MSL.

4. Discussion and conclusions

A distributed snow model has been applied to simulate the spatiotemporal evolution of the Austrian snow cover at 1 km × 1 km spatial and daily temporal resolution for the period 1948–2009. The comprehensive validation of the model on the basis of point-scale snow observations as well as remotely sensed snow distribution has revealed that the snow variables snow depth, snow distribution, and the number of SCDs can be reproduced with satisfying accuracy. A certain tendency for overestimation of snow depth in higher elevations and underestimation in lower elevations has been identified by comparison to observations at different station locations. While an elevation-dependent correction of snowfall might help to balance out part of this error, the applied calibration procedure has clearly shown that a uniform snow correction in space and time results in a most robust model performance. Moreover, the comparison of simulated snow coverage to the MODIS snow cover product has revealed no general tendency for overestimation of SCDs. For this important snow indicator, a ME of −4.8 and a MAE of 14.0 SCDs have been identified by comparing the simulated to observed SCDs at 22 station locations.

TABLE 4. Mean annual SCDs for the periods 1950–79 and 1980–2009 and four different subregions of Austria together with the change in SCDs comparing the conditions for both periods.

Region	1950–79	1980–2009	Change (SCDs)	Change (%)
Central Austria	141.0	128.4	−13	−9
Northeastern Austria	66.3	55.3	−11	−17
Southern Austria	143.9	128.8	−15	−10
Western Austria	165.6	152.6	−13	−8

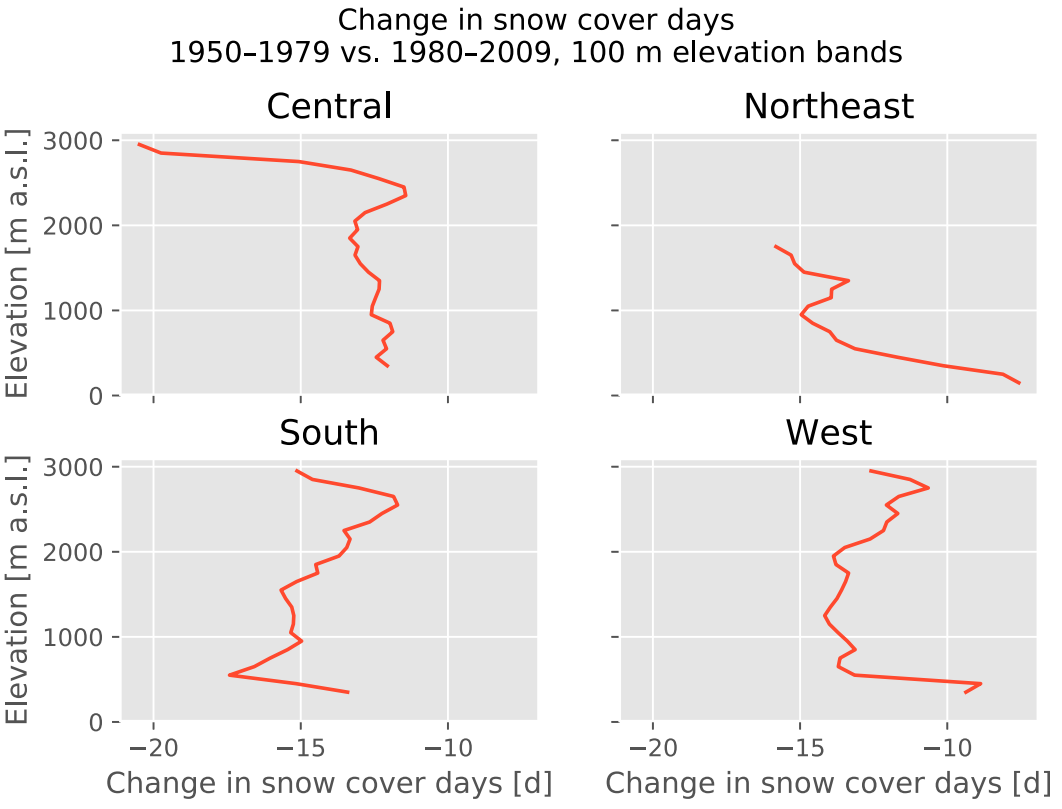

FIG. 7. Change in snow cover days for different elevation belts (width 100 m) and different subregions of Austria. Changes in elevations above 3000 m MSL are not included due to an insufficient number of raster cells in these elevations.

Comparing the SCDs simulated for the period 1980–2009 to those representing the years 1950–79 for all of Austria revealed a distinct decrease in SCDs, with a maximum of >35 SCDs near Villach (Carinthia). Station Villacher Alpe is the one with the lowest model performance in the reproduction of snow depth (see Table 3); hence, the results for this station are considered to be subject to high uncertainties. The analysis of SCD changes in different subregions of Austria has shown average changes ranging from −11 to −15 days. While these changes are well above the ME of −4.8 SCDs, they fall in the same range as the error margins of MAE (14 SCDs). The change from −11 to −15 SCDs only describes the mean conditions over all pixels in the different Austrian subregions, while the changes observed for the different elevation belts with up to −18 SCDs (500–2000 m) and over −20 SCDs (above 2500 m) exceed the error margins by far. Moreover, as can be observed by comparison of the values for ME and MEA, over- and underestimation to some degree cancel out and strongly reduce the overall bias. Finally, assuming that the biases in simulated SCDs are the same for the periods compared, considering the delta change (which other than the errors only points to one direction) is a valid approach for change detection followed in many climate change studies in the past (e.g., IPCC 2014).

While our findings with respect to the reduction of SCDs in midelevations are well in line with the findings of other studies carried out for the European (Hüsler et al. 2014), Swiss (Beniston 2012), and Italian Alps (Marcolini et al. 2017), the increased reduction of SCDs in higher elevations has not been reported so far. Comparing our results to those of Beniston (2012) and Marcolini et al. (2017), this could be explained by the fact that these studies considered only the winter season (defined there as the time from October to April and from November to April, respectively) where higher elevated mountain regions are often continuously snow covered in the early and recent past. This seems reasonable considering that the strongest decrease in SCDs above 1500 m MSL falls in the months of May to August, according to our model results. Hüsler et al. (2014), on the other hand, have analyzed a different period of time (1985–2011) applying a trend analysis rather than a delta change approach, making the results of their studies

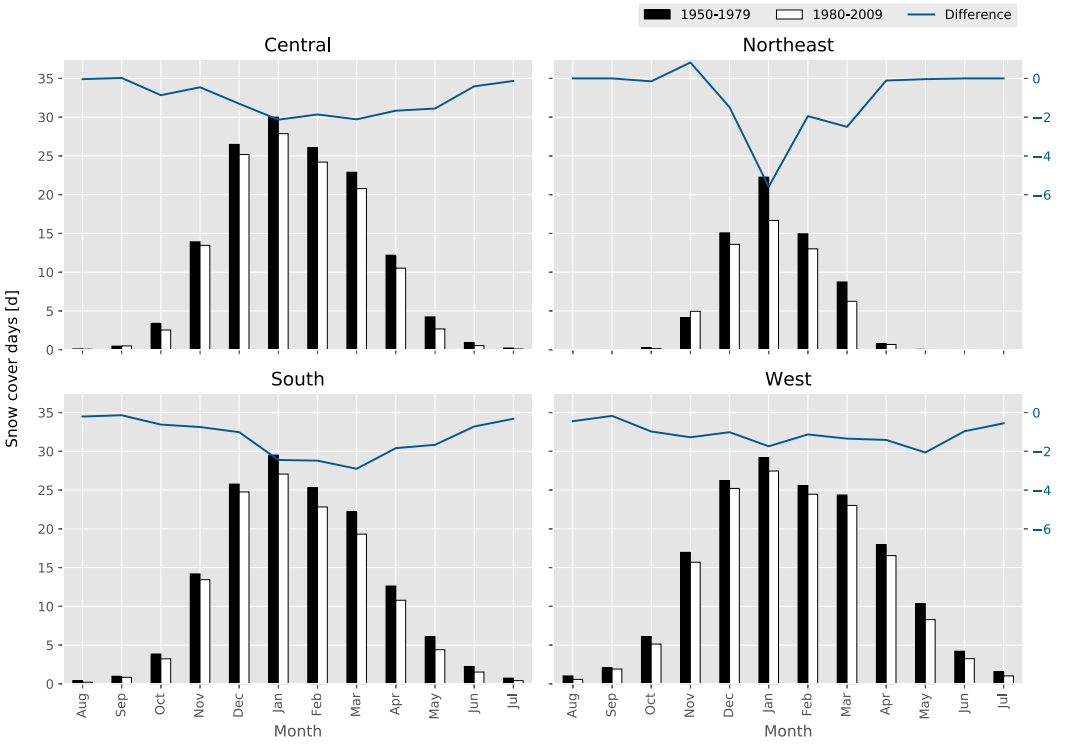

FIG. 8. Mean monthly snow cover days and change in snow cover days for the periods 1950–79 and 1980–2009 and four different subregions of Austria. The bars show the mean monthly snow cover days, and the blue line shows the change in snow cover days.

hard to compare to ours. This highlights a common problem in climate change–related snow studies: because of the strong decadal and interannual variability of the snow cover, existing studies considering different periods of time are hard to compare. This is even more true if differences exist also in the snow criteria analyzed, in the thresholds applied (e.g., to derive SCDs from snow depth or SWE), or in the approaches applied for change detection (trend analysis versus delta change approach).

Considering the temporal distribution of SCD change in the Austrian subregions as shown in our study, the decrease in SCDs seems to be rather due to a reduction in midwinter and at the end of winter than due to fewer SCDs in early winter. These findings are in agreement with those of Klein et al. (2016), who have identified earlier snowmelt as the reason for shorter snow cover duration in the Swiss Alps. The temporal distribution of SCD change in different elevation belts shows that at elevations below 1000 m MSL, the most distinct change in SCDs is due to a reduction of SCDs in January in most cases. Above 1000 m MSL, the most distinct change in SCDs is shifting toward the end of the winter season or even summer with increasing elevation. A maximum decrease in the months of June–August is observed at elevations above 2500 m MSL, which might be caused by a climate change–induced shift in the snow line. To prove this hypothesis, we have calculated the daily snow line for the period 1948–2009 as the elevation at which 50% of all raster cells are snow covered as proposed by Prantl et al. (2017). The daily snow lines have then been averaged for all months in the two time periods compared (1950–79 versus 1980–2009) to derive a mean monthly snow line for both periods and all months of the year. As Fig. 10 shows, a shift in the snow line can be observed in all Austrian subregions considered, with highest values of approximately 200 m found for southern and northeastern Austria in March and January, respectively.

The snow cover changes identified in our model results could be linked to anomalous warm winter temperatures in Europe in recent decades, which are reported to be unprecedented over the last 500 years (Luterbacher et al. 2007). Particularly the 1990s have been described as warm and dry in many recent studies (e.g., Brunetti et al. 2006, 2009) with respective consequences on snow conditions as well as snow precipitation. Beniston (1997) argues that pressure fields over the Alps have been far higher and more persistent since the mid-1980s compared to any other time in this century, resulting in a decrease of the snow season length as well as of snow amount. Comparing the influence of temperature and precipitation on SCD

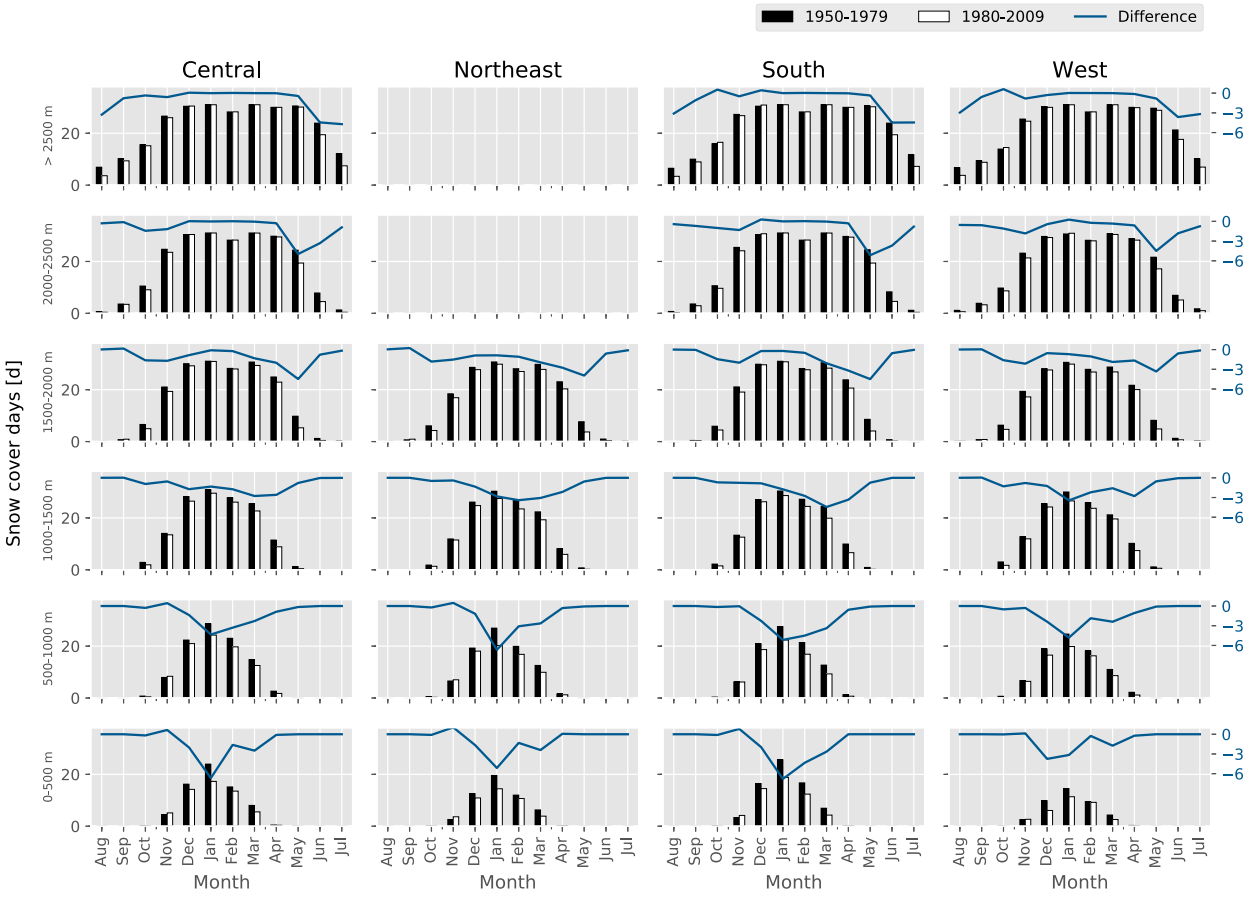

FIG. 9. Mean monthly snow cover days and change in snow cover days for the periods 1950–79 and 1980–2009 in different elevation belts of four different subregions of Austria. The bars show the mean monthly snow cover days, and the blue line shows the change in snow cover days.

decrease in Switzerland, Scherrer et al. (2004) found the increase in seasonal mean temperatures having larger influence than seasonal mean precipitation.

Other than studies analyzing long-term trends in snow cover days, the approach chosen in our study based on comparing long-term averages of snow cover days does not support a clarification whether the decrease in snow cover days is due to a decreasing trend or a step like change as observed by Marty (2008) for the Swiss Alps.

While the identified change in snow seasonality and amount can be expected to have direct and indirect implications for mountain ecosystems as well as economic consequences (Beniston et al. 2003b), the results of our study have to be interpreted keeping the model uncertainties and certain limitations of the applied approaches in mind. The pronounced change signal in high elevations is subject to a comparatively high degree of uncertainty. The latter arises from a combination of lateral snow transport processes that are not included in the present model setup, and large biases in precipitation recordings due to a wind-induced undercatch in the precipitation measurements. Moreover, all described changes in SCDs have to be interpreted with the background of a model-related uncertainty in the reproduction of past SCDs of −4.8 and 14.0 days for the two criteria of ME and MAE, respectively. Part of this uncertainty might be related to the simplified approach applied for the precipitation phase detection. As humidity measurements do not reach back far enough into the past, we have applied a temperature-based approach for precipitation phase detection. Harder and Pomeroy (2014) have investigated the effect of different precipitation phase partitioning methods on simulated snow conditions. They show that the uncertainty due to precipitation phase partitioning methods is largely a function of climate, vegetation, and topography, with a smaller influence of model complexity and catchment size. Differences between empirical and physically based methods vary with relative humidity and temperature. Because of the natural decrease in air temperature with increasing elevation, temperatures in lower elevations are often closer to the transition range, resulting in greater

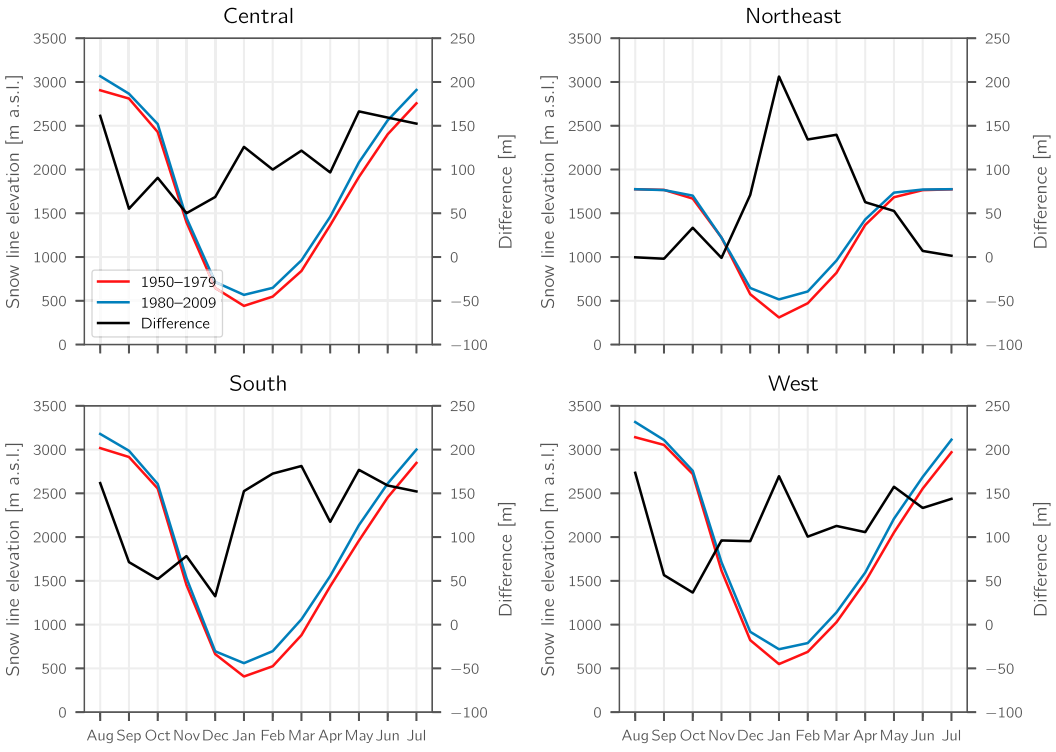

FIG. 10. Mean monthly elevation of the snow line for the periods 1950–79 and 1980–2009 and difference in the snow line elevation between the two periods.

uncertainty in precipitation phase determination based on temperature alone in lower elevations (Harder and Pomeroy 2014). While Harder and Pomeroy (2014) report that physically based methods in general are subject to smaller uncertainty, applying two thresholds for phase determination (with linear mixing of precipitation phase in between) compared to a single temperature threshold at least reduced the deviation from physically based methods from up to 33.2 days to a maximum of 11.2 days of snow cover duration in the four catchments considered in their study. To minimize the bias introduced by the simplified precipitation phase partitioning method applied (e.g., the bias introduced when the thresholds have been calibrated under conditions that differ from those of the model application), we calibrated the upper and lower limits for phase determination toward the best possible results for the region of application. Another uncertainty is that large parts of Austria are forest covered, but no snow–canopy interaction has been considered in the present model setup. While the applied snow model AMUNDSEN includes a submodel for modification of meteorological conditions and the simulation of snow–canopy interaction, this submodel has not been applied here because it requires the energy balance method for the calculation of the respective processes. It should be noted here that forests also affect the spatial validation based on the MODIS snow cover product, as the snow simulations are subject to certain biases induced by the missing consideration of snow–canopy interactions, whereas the accuracy of the MODIS snow cover product, on the other hand, is reported to be negatively affected in forested areas (Hall and Riggs 2007).

Following the limitations and uncertainties of the methods and data applied and discussed in this study, there are a number of potential activities to build upon the results of this study: 1) application of a more sophisticated spatial interpolation methodology of meteorological point measurements that is even better tailored to complex terrain (e.g., by attempting to consider regionally different vertical layering); 2) advanced in-depth trend analysis and validation of observed versus calculated snow cover for different time scales; 3) investigation and change detection of additional snow indicators related to snow depth, snow water equivalent, and fresh snow and heavy snowfall events (e.g., average and maximum snow depth, 24- or 72-h fresh snow amounts); 4) actualization of the analyzed period with more recent data becoming available; and 5) considering the effect of forests on the snow conditions in Austria. Many of these research aspects will be realized in a future study that is already in preparation.

Acknowledgments. The authors thank the Austrian Climate and Energy Fund for the financial support of the SNOWPAT project (ACRP4, B175124), which has facilitated this research within the Austrian Climate Research Programme. Moreover, we thank all contributors to this manuscript, particularly Marcel Siegmann for his continuous support in generating the numerous plots. Special thanks also go to Klaus Niedertscheider from the Hydrographical Service of Tyrol for his continuous support. Thomas Marke and Ulrich Strasser conceived and designed the modeling experiments and developed the original model, Florian Hanzer adapted the snow model and performed all model simulations, Marc Olefs provided expertise in interpreting the model results, and Thomas Marke wrote the largest parts of the manuscript.

REFERENCES

APCC, 2014: Austrian Assessment Report Climate Change 2014 (AAR14): Synopsis – Main Findings. Climate Change Centre Austria, 12 pp., https://www.ccca.ac.at/fileadmin/00_DokumenteHauptmenue/03_Aktivitaeten/APCC/summarys/Synopse_englisch_finaleversion_181214.pdf.

Auer, I., J. Nemec, C. Gruber, B. Chimani, and K. Türk, 2010: HOM-START: Homogenisation of climate series on a daily basis, an application to the StartClim dataset. Climate and Energy Fund Project Rep., 34 pp., https://www.zamg.ac.at/cms/de/dokumente/klima/dok_projekte/homstart/homstart-endbericht.

Barnett, T. P., J. C. Adam, and D. P. Lettenmaier, 2005: Potential impacts of a warming climate on water availability in snow-dominated regions. *Nature*, **438**, 303–309, https://doi.org/10.1038/nature04141.

Beniston, M., 1997: Variations of snow depth and duration in the Swiss Alps over the last 50 years: Links to changes in large-scale climatic forcings. *Climatic Change*, **36**, 281–300, https://doi.org/10.1023/A:1005310214361.

——, 2012: Is snow in the Alps receding or disappearing? *Wiley Interdiscip. Rev. Climate Change*, **3**, 349–358, https://doi.org/10.1002/wcc.179.

——, F. Keller, and S. Goyette, 2003a: Snow pack in the Swiss Alps under changing climatic conditions: An empirical approach for climate impacts studies. *Theor. Appl. Climatol.*, **74**, 19–31, https://doi.org/10.1007/s00704-002-0709-1.

——, ——, B. Koffi, and S. Goyette, 2003b: Estimates of snow accumulation and volume in the Swiss Alps under changing climatic conditions. *Theor. Appl. Climatol.*, **76**, 125–140, https://doi.org/10.1007/s00704-003-0016-5.

Brunetti, M., M. Maugeri, T. Nanni, I. Auer, R. Böhm, and W. Schöner, 2006: Precipitation variability and changes in the Greater Alpine Region over the 1800–2003 period. *J. Geophys. Res.*, **111**, 1–29, https://doi.org/10.1029/2005JD006674.

——, G. Lentini, M. Maugeri, T. Nanni, I. Auer, R. Böhm, and W. Schöner, 2009: Climate variability and change in the Greater Alpine Region over the last two centuries based on multi-variable analysis. *Int. J. Climatol.*, **29**, 2197–2225, https://doi.org/10.1002/joc.1857.

EEA, 2012: Climate change, impacts and vulnerability in Europe 2012—An indicator-based report. EEA Rep. 12/2012, 304 pp., https://www.eea.europa.eu/publications/climate-impacts-and-vulnerability-2012.

Hall, D. K., and G. A. Riggs, 2007: Accuracy assessment of the MODIS snow products. *Hydrol. Processes*, **21**, 1534–1547, https://doi.org/10.1002/hyp.6715.

——, ——, V. V. Solomonson, N. E. DiGirolamo, and K. J. Bayr, 2002: MODIS snow-cover products. *Remote Sens. Environ.*, **83**, 181–194, https://doi.org/10.1016/S0034-4257(02)00095-0.

Hantel, M., M. Ehrendorfer, and A. Haslinger, 2000: Climate sensitivity of snow cover duration in Austria. *Int. J. Climatol.*, **20**, 615–640, https://doi.org/10.1002/(SICI)1097-0088(200005)20:6<615::AID-JOC489>3.0.CO;2-0.

Hanzer, F., K. Helfricht, T. Marke, and U. Strasser, 2016: Multilevel spatiotemporal validation of snow/ice mass balance and runoff modeling in glacierized catchments. *Cryosphere*, **10**, 1859–1881, https://doi.org/10.5194/tc-10-1859-2016.

Harder, P., and J. Pomeroy, 2014: Hydrological model uncertainty due to precipitation-phase partitioning methods. *Hydrol. Processes*, **28**, 4311–4327, https://doi.org/10.1002/hyp.10214.

Harpold, A. A., M. L. Kaplan, P. Z. Klos, T. Link, J. P. McNamara, S. Rajagopal, R. Schumer, and C. M. Steele, 2017: Rain or snow: Hydrologic processes, observations, prediction, and research needs. *Hydrol. Earth Syst. Sci.*, **21**, 1–22, https://doi.org/10.5194/hess-21-1-2017.

Hinzman, L. D., D. L. Kane, C. S. Benson, and K. R. Everett, 1996: Energy balance and hydrological processes in an Arctic watershed. *Landscape Function: Implications for Ecosystem Response to Disturbance: A Case Study in Arctic Tundra*, Ecological Studies Series, Vol. 120, Springer, 131–154, https://doi.org/10.1007/978-3-662-01145-4_6.

Hüsler, F., T. Jonas, M. Riffler, J. P. Musial, and S. Wunderle, 2014: A satellite-based snow cover climatology (1985–2011) for the European Alps derived from AVHRR data. *Cryosphere*, **8**, 73–90, https://doi.org/10.5194/tc-8-73-2014.

IPCC, 2014: *Climate Change 2014: Synthesis Report*. IPCC, 151 pp.

Jin, J., and N. L. Miller, 2007: Analysis of the impact of snow on daily weather variability in mountainous regions using MM5. *J. Hydrometeor.*, **8**, 245–258, https://doi.org/10.1175/JHM565.1.

Kane, D., L. D. Hinzman, C. S. Benson, and G. E. Liston, 1991: Snow hydrology of a headwater Arctic basin. 1. Physical measurements and process studies. *Water Resour. Res.*, **27**, 1099–1109, https://doi.org/10.1029/91WR00262.

Keller, F., S. Goyette, and M. Beniston, 2005: Sensitivity analysis of snow cover to climate change scenarios and their impact on plant habitats in Alpine terrain. *Climatic Change*, **72**, 299–319, https://doi.org/10.1007/s10584-005-5360-2.

Klein, G., Y. Vitasse, C. Rixen, C. Marty, and M. Rebetez, 2016: Shorter snow cover duration since 1970 in the Swiss Alps due to earlier snowmelt more than to later snow onset. *Climatic Change*, **139**, 637–649, https://doi.org/10.1007/s10584-016-1806-y.

Kottek, M., J. Grieser, C. Beck, B. Rudolf, and F. Rubel, 2006: World map of the Köppen-Geiger climate classification updated. *Meteor. Z.*, **15**, 259–263, https://doi.org/10.1127/0941-2948/2006/0130.

Krause, P., D. P. Boyle, and F. Bäse, 2005: Comparison of different efficiency criteria for hydrological model assessment. *Adv. Geosci.*, **5**, 89–97, https://doi.org/10.5194/adgeo-5-89-2005.

Laternser, M., and M. Schneebeli, 2003: Long-term snow climate trends of the Swiss Alps (1931–99). *Int. J. Climatol.*, **23**, 733–750, https://doi.org/10.1002/joc.912.

Liston, G. E., and K. Elder, 2006: A meteorological distribution system for high-resolution terrestrial modeling (MicroMet). *J. Hydrometeor.*, **7**, 217–234, https://doi.org/10.1175/JHM486.1.

Luce, C. H., D. G. Tarboton, and K. R. Cooley, 1998: The influence of the spatial distribution of snow on basin-averaged snowmelt. *Hydrol. Processes*, **12**, 1671–1683, https://doi.org/10.1002/(SICI)1099-1085(199808/09)12:10/11<1671::AID-HYP688>3.0.CO;2-N.

Luterbacher, J. M., A. Liniger, A. Menzel, N. Estrella, P. M. Della-Marta, C. Pfister, T. Rutishauser, and E. Xoplaki, 2007: Exceptional European warmth of autumn 2006 and winter 2007: Historical context, the underlying dynamics, and its phenological impacts. *Geophys. Res. Lett.*, **34**, L12704, https://doi.org/10.1029/2007GL029951.

Marcolini, G., A. Bellin, M. Disse, and G. Chiogna, 2017: Variability in snow depth time series in the Adige catchment. *J. Hydrol. Reg. Stud.*, **13**, 240–254, https://doi.org/10.1016/j.ejrh.2017.08.007.

Marke, T., 2008: Development and application of a model interface to couple land surface models with regional climate models for climate change risk assessment in the upper Danube watershed. Ph.D. thesis, Ludwig-Maximilians-University, 220 pp., https://edoc.ub.uni-muenchen.de/9162/.

——, U. Strasser, F. Hanzer, J. Stötter, R. A. I. Wilcke, and A. Gobiet, 2015: Scenarios of future snow conditions in Styria (Austrian Alps). *J. Hydrometeor.*, **16**, 261–277, https://doi.org/10.1175/JHM-D-14-0035.1.

Marsh, P., 1999: Snowcover formation and melt: Recent advances and future prospects. *Hydrol. Processes*, **13**, 2117–2134, https://doi.org/10.1002/(SICI)1099-1085(199910)13:14/15<2117::AID-HYP869>3.0.CO;2-9.

Marty, C., 2008: Regime shift of snow days in Switzerland. *Geophys. Res. Lett.*, **35**, L12501, https://doi.org/10.1029/2008GL033998.

——, A.-M. Tilg, and T. Jonas, 2017: Recent evidence of large-scale receding snow water equivalents in the European Alps. *J. Hydrometeor.*, **18**, 1021–1031, https://doi.org/10.1175/JHM-D-16-0188.1.

Nemec, J., C. Gruber, B. Chimani, and I. Auer, 2013: Trends in extreme temperature indices in Austria based on a new homogenised dataset of daily minimum and maximum temperature series. *Int. J. Climatol.*, **33**, 1538–1550, https://doi.org/10.1002/joc.3532.

Parajka, J., and G. Blöschl, 2006: Validation of MODIS snow cover images over Austria. *Hydrol. Earth Syst. Sci.*, **10**, 679–689, https://doi.org/10.5194/hess-10-679-2006.

——, and ——, 2008a: Spatio-temporal combination of MODIS images— Potential for snow cover mapping. *Water Resour. Res.*, **44**, W03406, https://doi.org/10.1029/2007WR006204.

——, and ——, 2008b: The value of MODIS snow cover data in validating and calibrating conceptual hydrologic models. *J. Hydrol.*, **358**, 240–258, https://doi.org/10.1016/j.jhydrol.2008.06.006.

Pellicciotti, F., B. Brock, U. Strasser, P. Burlando, M. Funk, and J. Corripio, 2005: An enhanced temperature-index glacier melt model including the shortwave radiation balance: Development and testing for Haut Glacier d'Arolla, Switzerland. *J. Glaciol.*, **51**, 573–587, https://doi.org/10.3189/172756505781829124.

Prantl, H., L. Nicholson, R. Sailer, F. Hanzer, I. F. Juen, and P. Rastner, 2017: Glacier snowline determination from terrestrial laser scanning intensity data. *Geosciences*, **7**, 60, https://doi.org/10.3390/geosciences7030060.

Richter, K., T. B. Hank, W. Mauser, and C. Atzberger, 2012: Derivation of biophysical variables from Earth observation data: Validation and statistical measures. *J. Appl. Remote Sens.*, **6**, 063557, https://doi.org/10.1117/1.JRS.6.063557.

Rittger, K., T. H. Painter, and J. Dozier, 2013: Assessment of methods for mapping snow cover from MODIS. *Adv. Water Resour.*, **51**, 367–380, https://doi.org/10.1016/j.advwatres.2012.03.002.

Rohrer, M. B., 1992: Die Schneedecke im Schweizer Alpenraum und ihre Modellierung. *Zuricher Geogr. Schriften*, **49**, 178.

Scherrer, S. C., C. Appenzeller, and M. Laternser, 2004: Trends in Swiss Alpine snow days: The role of local- and large-scale climate variability. *Geophys. Res. Lett.*, **31**, L13215, https://doi.org/10.1029/2004GL020255.

Schöner, W., I. Auer, and R. Böhm, 2009: Long term trend of snow depth at Sonnblick (Austrian Alps) and its relation to climate change. *Hydrol. Processes*, **23**, 1052–1063, https://doi.org/10.1002/hyp.7209.

Serquet, G., C. Marty, J. P. Dulex, and M. Rebetez, 2011: Seasonal trends and temperature dependence of the snowfall/precipitation-day ratio in Switzerland. *Geophys. Res. Lett.*, **38**, L07703, https://doi.org/10.1029/2011GL046976.

Strasser, U., 2008: Modelling of the mountain snow cover in the Berchtesgaden National Park. Forschungsberichte des Nationalpark Berchtesgaden 55, 104 pp.

——, J. G. Corripio, B. Brock, F. Pellicciotti, P. Burlando, and M. Funk, 2004: Spatial and temporal variability of meteorological variables at Haut Glacier d'Arolla (Switzerland) during the ablation season 2001: Measurements and simulations. *J. Geophys. Res.*, **109**, D03103, https://doi.org/10.1029/2003JD003973.

——, M. Bernhardt, M. Weber, G. E. Liston, and W. Mauser, 2008: Is snow sublimation important in the alpine water balance? *Cryosphere*, **2**, 53–66, https://doi.org/10.5194/tc-2-53-2008.

Thornton, P. W., S. W. Running, and M. A. White, 1997: Generating surfaces of daily meteorological variables over large regions of complex terrain. *J. Hydrol.*, **190**, 214–251, https://doi.org/10.1016/S0022-1694(96)03128-9.

Zappa, M., 2008: Objective quantitative spatial verification of distributed snow cover simulations—An experiment for the whole of Switzerland. *Hydrol. Sci. J.*, **53**, 179–191, https://doi.org/10.1623/hysj.53.1.179.